

## FEDSM-ICNMM2010-' \$\* ( \*

### COUPLED ANALYSIS OF UNSTEADY AERODYNAMICS AND VEHICLE MOTION OF A HEAVY DUTY TRUCK IN WIND GUSTS

**Takuji Nakashima**

Hiroshima University  
Higashi-Hiroshima, Hiroshima, Japan

**Makoto Tsubokura**

Hokkaido University  
Sapporo, Hokkaido, Japan

**Takeshi Ikenaga**

Hiroshima University  
Higashi-Hiroshima, Hiroshima, Japan

**Kozo Kitoh**

Kozo Kitoh Technology, Inc.  
Shibuya, Tokyo, Japan

**Yasuaki Doi**

Hiroshima University  
Higashi-Hiroshima, Hiroshima, Japan

#### ABSTRACT

In the present study, unsteady aerodynamic forces acting on a simplified heavy duty truck in strong wind gust and their effects on the truck's motion were investigated by using a coupled analysis. Unsteady fluid dynamics simulation was applied to numerically reproduce unsteady aerodynamic forces acting on the truck under sudden crosswind condition. Taking account of vehicle's motion, moving boundary techniques were introduced. Motions of the truck were simulated by a vehicle dynamics simulation including a driver's reaction. The equations of motion of the truck in longitudinal, lateral, and yaw-rotational directions were numerically solved. These aerodynamics and vehicle dynamics simulations were coupled by exchanging the aerodynamic forces and the vehicle's motion. In order to investigate effects of the unsteady vehicle aerodynamics on the vehicle's motion, conventional analysis of the vehicle's motion using quasi-steady aerodynamic forces and one-way coupled analysis with fixed vehicle attitude were also conducted. The numerical results of these simulations were compared with each other, and the effects of the two kinds of unsteady aerodynamics were discussed separately and totally. In the sudden crosswind condition, the unsteady aerodynamics effected significantly on the truck's motion. An effect of transient aerodynamics as the truck ran into a sudden crosswind was greater than an effect of unsteady aerodynamics caused by

unsteady vehicle's motion, while both of the effects showed significance.

#### INTRODUCTION

In recent years, unsteady vehicle aerodynamics under real driving conditions has attracted much attention. Many research groups (1-3) in a field of vehicle aerodynamics research have reported the importance of unsteady aerodynamics. One of the typical phenomena regarding such unsteady aerodynamics of vehicle is a sudden crosswind. A number of researches of vehicle aerodynamics under sudden crosswind conditions (4-6) have been conducted for the last several decades. For example, the significant unsteadiness of aerodynamic forces acting on a vehicle subjects to sudden crosswind have been reported (5). However, the effects of such unsteady aerodynamics on vehicle's motion have not been clarified quantitatively enough. In vehicle dynamics research today (7), aerodynamic forces are still considered quasi-steadily, because the unsteady aerodynamics is difficult to estimate, especially in a design process before a real vehicle has been produced.

Therefore, the purpose of this study is to investigate how unsteady aerodynamic forces act on a vehicle subjects to a sudden crosswind, and how such transient forces affect the running or driving stability of the vehicle. Coupled numerical simulation of unsteady aerodynamics and vehicle dynamics was applied to a heavy duty truck subjects to a sudden crosswind.

An importance of the unsteady aerodynamics of commercial trucks is greater than the one of general passenger car. It is explained by considering the large lateral area and aspect ratio of the long body of a truck, which enhance the effect of unsteady aerodynamic forces and moments of crosswind.

As a numerical technique for the coupled simulation, large-eddy simulation (LES) for unsteady aerodynamics simulation with moving boundary techniques and vehicle dynamics simulation with a driver's reaction model were simultaneously conducted and fully coupled with each other. The LES technique for turbulence modeling is more suitable than conventional method based on the Reynolds averaged Navier–Stokes equations, because LES is a fundamentally unsteady modeling approach for turbulence. The vehicle dynamics simulation was conducted by using the aerodynamic force and moment calculated in the LES. On the other hand, vehicle's motion simulated in the vehicle dynamics simulation was taken into account in the LES by applying the moving boundary techniques. In order to extract effects of unsteady aerodynamics on vehicle's motion, the fully coupled simulation results were compared with another types of simulations based on quasi-steady aerodynamics or one-way coupled simulation with fixed vehicle attitude. Comparing aerodynamic forces and vehicle motions predicted in these simulations, effects of the unsteady aerodynamics on vehicle's motion were discussed totally and separately. A transient aerodynamics when the truck ran into the crosswind and unsteady aerodynamics caused by a unsteady motion of the truck were investigated and discussed.

## NOMENCLATURE

- $\bar{\quad}$  (Overbar) : A spatially filtered value.
- $A$  : An angle of the steering wheel [deg.].
- $C$  : An equivalent damping coefficient of a steering system [N m s/rad].
- $C_p$  : A pressure coefficient [-].
- $C_{Sm}$  : A model coefficient of Smagorinsky model for SGS turbulence model [-].
- $C_S$  : A lateral force coefficient of the vehicle [-].
- $C_{ym}$  : A yawing moment coefficient of the vehicle [-].
- $l_f, l_m, l_r$  : Distances from the gravity center to front, middle, and rear axles of the vehicle [m], respectively.
- $d_f, d_m, d_r$  : Wheel tracks of front, middle, and rear axles of the vehicle [m], respectively.
- $F_d$  : Steering force of a driver [N]. ( $F_d = H\epsilon$ )
- $Fx_{ij}, Fy_{ij}$  : Tire forces [N] in longitudinal and lateral directions of the tire. The subscript  $i$  indicates the front, middle, and rear axles and the subscript  $j$  indicates the left and right tires. For example,  $Fx_{1l}$  is longitudinal force on a front left tire and  $Fy_{3r}$  is lateral force on a rear right tire.
- $Fx'_{ij}, Fy'_{ij}$  : Tire forces [N] in longitudinal and lateral directions of the vehicle. Definitions of the subscripts are the same as  $Fx_{ij}$  and  $Fy_{ij}$ .
- $F_w$  : Aerodynamic lateral force acting on the vehicle [N].

- $f_{ri}$  : Inertial force on a non-inertial reference frame in  $i$ -th direction [m/s<sup>2</sup>].
- $H$  : Model constant of a driver's reaction model [N].
- $I$  : Equivalent inertia moment of the steering system [kg m<sup>2</sup>/rad].
- $I_z$  : Inertia moment of the vehicle around its gravity center [kg m<sup>2</sup>].
- $K_{st}$  : Equivalent elastic coefficient of the steering system.
- $L_{wheel}$  : Wheelbase of a vehicle [m]
- $M_w$  : Aerodynamic yaw moment acting on a vehicle [Nm].
- $n$  : The inverse of steering ratio [-].
- $\bar{P}$  : Spatially filtered pressure;  $\bar{P} = \bar{p}/\rho + 1/3(\overline{u_i u_i} - \overline{u_i} \overline{u_i})$ .
- $p$  : Pressure [Pa].
- $r$  : Radius of the steering wheel [m].
- $\bar{S}_{ij}$  : Spatially filtered strain tensor;  $\bar{S}_{ij} = 1/2(\partial \bar{u}_j / \partial x_i + \partial \bar{u}_i / \partial x_j)$ .
- $S$  : The frontal area of the vehicle [m<sup>2</sup>].
- $u_i$  : Flow velocity in  $i$ -th direction [m/s].
- $u_{gi}$  : Grid deformation velocity in  $i$ -th direction [m/s].
- $t$  : Time [s].
- $T_r$  : Time interval for a delay of human reaction [s].
- $T_{SA}$  : Self aligning torque of the tire [Nm].
- $U$  : Longitudinal velocity of the vehicle [m/s].
- $V$  : Lateral velocity of the vehicle [m/s].
- $V_{CW}$  : Crosswind velocity [m/s].
- $V_{CW,max}$  : The maximum crosswind velocity [m/s].
- $V_R$  : Relative velocity between the air and a vehicle [m/s].
- $x_i$  : Coordinates in  $i$ -th direction on a non-inertial reference frame for the fluid dynamics simulation [m].
- $X, Y$  : Absolute coordinates of vehicle's gravity center [m].
- $y^+$  : Wall distance [-].
- $\beta_w$  : Aerodynamic yaw angle [rad.].
- $\delta$  : Steering angle of front wheels of the vehicle [rad.].
- $\nu$  : Dynamic viscosity of the air [m<sup>2</sup>/s].
- $\nu_{SGS}$  : Sub-grid scale eddy viscosity [m<sup>2</sup>/s].
- $\Psi$  : Yaw angle of the vehicle [rad.].
- $\epsilon$  : Predictable course deviation [m].
- $\tau$  : Predictable time [s].

## TARGET TRUCK AND CONDITIONS

As target vehicle geometry, a simplified truck model developed in our previous study (8) was adopted. This geometry was based on a real commercial truck and its details, such as small parts, was removed from the body to reduce computational cost for a coupled simulation of unsteady aerodynamics and vehicle's motion. The steady aerodynamics of the simplified truck was validated by comparisons with the aerodynamics of a real heavy duty truck under the same conditions (8). Orthogonal views of the simplified geometry are shown in Fig.1. The weight of the simplified truck was set to be 9,000 kg under no-load condition. The mechanical characteristics of suspension and damper were determined from the characteristics of the original commercial truck.

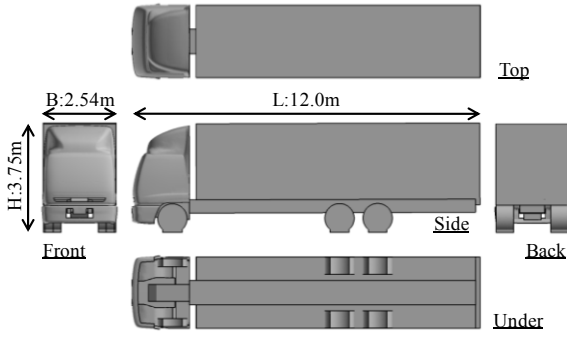


**Fig. 1 Orthogonal views of the target truck with a simplified geometry**

### Coordinate Systems

Figure 2 shows definitions of coordinate systems for present numerical simulations of fluid dynamics and vehicle dynamics.

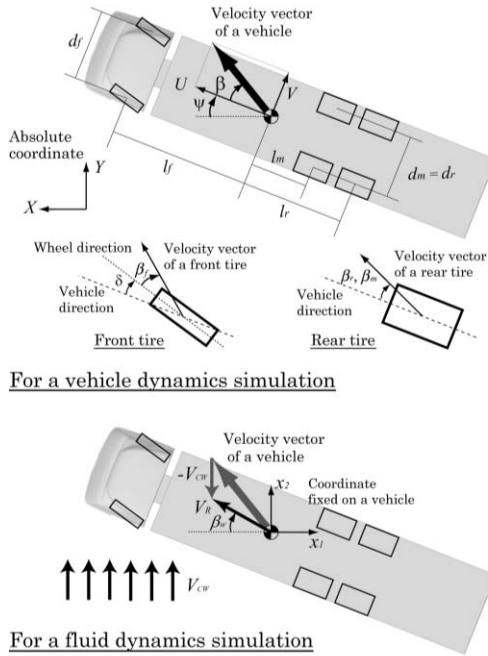


**Fig. 2 Definition of variables for vehicle dynamics simulation.**

### Target Conditions

As a running condition of the target truck, a constant running speed was assumed to be 25.1 m/s. The Reynolds number based on the running speed and the length of the truck was  $2.0 \times 10^7$ . A straight track was set in X direction as  $Y = 0$  and a gusty crosswind region with step-like velocity profile was allocated on the track as a disturbance. Width of the crosswind region was 50.3 m and the velocity profile is shown in Fig.3. The time-series of crosswind velocity was obtained in the present numerical simulation at a point above the gravity center of the truck, as shown in Fig.3. The maximum crosswind

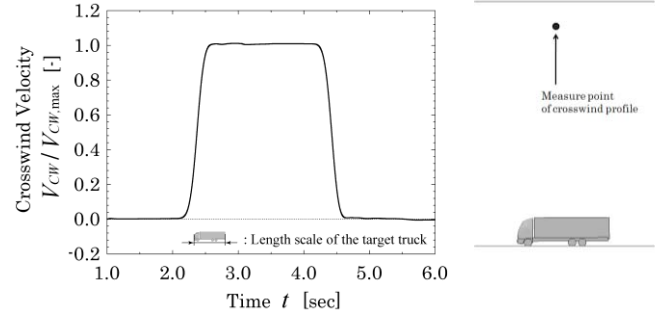


**Fig.3 Crosswind profile and its measure point.**

velocity is defined as the same value as the constant running speed of the truck and the aerodynamic yaw angle becomes 45 degrees.

### GOVERNING EQUATION

For the coupled simulation of fluid dynamics around the truck and vehicle dynamics of the truck, the governing equations of each dynamics were numerically analyzed and they were coupled by exchanging the aerodynamic forces and the vehicle's attitude at every time-step of both the simulations.

### Fluid Dynamics

For the fluid dynamics simulation, a non-inertial reference frame fixed on the vehicle was adopted to represent vehicle's translational motion. Then, a rotational motion of the vehicle was reproduced by the deformation of the computational grid. The governing equations for a large-eddy simulation with incompressible assumption become the spatially filtered conservation equation of mass and momentum. Considering the inertial force on the referenced frame and the velocity of grid-deformation based on the Arbitrary Lagrangian-Eulerian (ALE) method (9), the governing equations assuming sub-grid scale (SGS) turbulent eddy viscosity become as follows;

$$\frac{\partial \bar{u}_i}{\partial x_i} = 0 \quad (1)$$

$$\frac{\partial \bar{u}_i}{\partial t} + \frac{\partial}{\partial x_j} (\bar{u}_i - u_g) \bar{u}_j = -\frac{\partial \bar{P}}{\partial x_i} + 2 \frac{\partial}{\partial x_j} (\nu + \nu_{SGS}) \bar{S}_{ij} - f_{ri} \quad (2)$$

The sub-grid scale eddy viscosity  $\nu_{SGS}$  in equation 2 must be modeled by an SGS turbulent model, and the standard Smagorinsky model (10)

$$\nu_{SGS} = (C_{Sm} f_d \Delta)^2 \sqrt{2 \bar{S}_{ij} \bar{S}_{ij}} \quad (3)$$

is applied in the present simulation. Here, the model constant  $C_{Sm}$  is set to be 0.15, which is a generally suitable value for external flows. The damping of the turbulent effect near a wall boundary is explained by the Van Driest-type damping function as follows:

$$f_d = 1 - \exp(-y^+ / 26) \quad (4)$$

## Vehicle Dynamics

For a vehicle dynamics simulation, we adopted governing equations that had been introduced and validated for a vehicle motion of a compact car by Maruyama *et al.* (7). In the present study, the evaluation of aerodynamics was extended by using unsteady aerodynamic force and moment predicted by the LES.

### Motion Equations

To simplify the problem, vertical motion of the truck was neglected and the pitching and rolling motion assumed to be balanced statically. Then, only the horizontal motion of the vehicle was treated. The equations of motion in the longitudinal, lateral, and yaw-rotation directions of the vehicle becomes

$$m\left(\frac{dU}{dt} - V\frac{d\psi}{dt}\right) = \sum_i \sum_j (Fx_{ij} \cos \delta - Fy_{ij} \sin \delta) = \sum_{i,j} Fx'_{ij}, \quad (5)$$

$$m\left(\frac{dV}{dt} + U\frac{d\psi}{dt}\right) = \sum_i \sum_j (Fx_{ij} \sin \delta + Fy_{ij} \cos \delta) + F_w = \sum_{i,j} Fy'_{ij} + F_w, \quad (6)$$

$$I_z \frac{d^2\psi}{dt^2} = (Fy'_{11} + Fy'_{12})l_f + (Fx'_{11} - Fx'_{12})\frac{d_f}{2} - (Fy'_{21} + Fy'_{22})l_m + (Fx'_{21} - Fx'_{22})\frac{d_m}{2} - (Fy'_{31} + Fy'_{32})l_r + (Fx'_{31} - Fx'_{32})\frac{d_r}{2} + M_w, \quad (7)$$

respectively. The tire forces in their lateral direction  $Fy_{ij}$  depend on load and side-slip angle, and their relations were determined by referencing the experimental database of the real tire for a heavy duty truck. Here, the loads on tire were calculated from the mass of the truck and the static balances in its pitch and roll directions. Their sideslip angles were calculated from  $U$ ,  $V$ ,  $\psi$ , and  $\delta$ . The steering angle of front tire  $\delta$  was calculated by the motion equation of the steering system with a driver's reaction model, which are described below.

On the other hand, it is assumed that the driver only controls the steering and does not control the acceleration for simplicity. Based on this assumption, the tire forces in its longitudinal direction  $Fx_{ij}$  were assumed more simply to be zero.

### Driver's Reaction Model and Steering System

In order to represent a driver's reaction when the truck runs off the track, the second-order predictable correction model proposed by Yoshimoto (11) was adopted to determine a steering action of the driver. In this model, the lateral position of the vehicle after  $\tau$  seconds  $Y(t + \tau)$  is evaluated from the position, velocity, and acceleration of the vehicle at the present time  $t$ :

$$Y(t + \tau) = Y(t) + \frac{d}{dt}Y(t) \cdot \tau + \frac{1}{2!} \frac{d^2}{dt^2}Y(t) \cdot \tau^2. \quad (8)$$

The driver's reaction appears as a steering force  $F_d$  to correct the course and  $F_d$  is proportional to the predictable course deviation  $\varepsilon$  with proportionality factor  $H$ :  $F_d = H\varepsilon$ . In this study, a predictable course deviation  $\varepsilon$  becomes  $Y(t + \tau)$  because the straight track  $Y=0$  was assumed. To represent a time delay in human reaction, the reaction is assumed to be discrete (11) and the steering force was evaluated at interval of  $T_r$  seconds.

The steering force is substitute into a rotational motion equation of a steering system given as follows:

$$nI \frac{d^2 A}{dt^2} + nC \frac{dA}{dt} + K_{st}(nA - \delta) = \frac{F_d r}{n}. \quad (9)$$

Finally, the steering angle of the front wheel is evaluated as follows:

$$\delta = \frac{2T_{SA}}{K_{st}} + nA. \quad (10)$$

Here,  $T_{SA}$  was also determined by the function of the load and the sideslip angle as well as the tire force in its lateral direction.

## NUMERICAL SETUP AND METHODS

### Fluid Dynamics Simulation

#### Boundary Conditions

The computational domain was defined as a rectangular duct shown in Fig.4. A uniform streamwise and lateral velocities, which represent the relative velocity between still air and a vehicle motion, were imposed on the front and side boundaries of the domain as a Dirichlet condition. Both streamwise and lateral velocities were time varying and their variations were given by the translational vehicle motion calculated in the motion equation at every time step. In order to reproduce sudden crosswind acting on the track, a crosswind profile mentioned above was added to the uniform velocity in the lateral direction and the combined velocity profile convects with the streamwise velocity. Details of this numerical technique to reproduce sudden crosswind conditions were given in our previous reports (12, 13). Top and bottom boundaries of the domain were treated as free-slip wall and a downstream boundary behind the truck was treated as a free-outlet boundary with a gradient-free condition.

#### Numerical Schemes and Analysis Software

The governing equations are spatially discretized by a vertex-centered unstructured finite volume method. The SMAC algorithm was employed for the pressure-velocity coupling. A second-order central difference scheme was applied for the spatial derivative and blended with 5% convective flux of a first-order upwind scheme for the convective term in the

## Vehicle Dynamics Simulation

### Numerical Schemes

The fourth-order Runge–Kutta method was adopted for the numerical integration of the governing equations 5, 6, and 7. The equation 9 for a steering system was also numerically integrated by the same method. The discretized time period was  $5.0 \times 10^{-5}$  s, as in the aerodynamics simulations.

### Model Parameters

The parameters of the truck, such as geometry, mass, and inertia moment, were given by characteristics of the simplified truck model, which was developed from the real heavy duty truck. The parameters of the steering system were obtained by upscaling and modifying parameters for a compact car used by Maruyama *et al.* (7). On the basis of general values of the steering radius and steering ratio, the equivalent inertia moment and the equivalent damping coefficient are set to be 4.8 times the values for the compact car. The equivalent elastic coefficient is twice that of the compact car. The parameters of the driver's reaction model are set as the same values used in Maruyama *et al.* (7). Evaluation of driver's reaction began when the course deviation  $\varepsilon$  became larger than 0.5 m. The parameter values are listed in Table 1.

**Table 1. Parameters for the dynamics of a steering system and a driver's reaction model**

| Parameter                     | Value             |
|-------------------------------|-------------------|
| $r$ [m]                       | 0.24              |
| $n$ [-]                       | 0.032 (=1/31)     |
| $I$ [N m s <sup>2</sup> /rad] | $5.7 \times 10^1$ |
| $C$ [N m s/rad]               | $4.2 \times 10^3$ |
| $K_{st}$ [N m/rad]            | $9.7 \times 10^4$ |
| $H$ [N]                       | 3.9               |
| $\tau$ [s]                    | 2.0               |
| $T$ [s]                       | 0.60              |

### Coupling Methods between the Fluid and Vehicle Dynamics Simulations

The numerical simulations of fluid dynamics and vehicle dynamics were conducted with the same time interval of the discretizations, as previously described. Their results are explicitly exchanged with each other at every time step.

### Evaluation of Vehicle Motion in the Fluid Dynamics Simulation

In the fluid dynamics simulation, the inertial forces  $f_{ri}$  in  $X$  and  $Y$  directions are given by the motion equation of the vehicle. They are opposed in sign to the translational accelerations of the vehicle, which are in the left hand side of equations 5 and 6 of the motion equations of the vehicle.

Yaw angle of the truck and the angular rate are also given by the motion equation and they are reproduced in the fluid

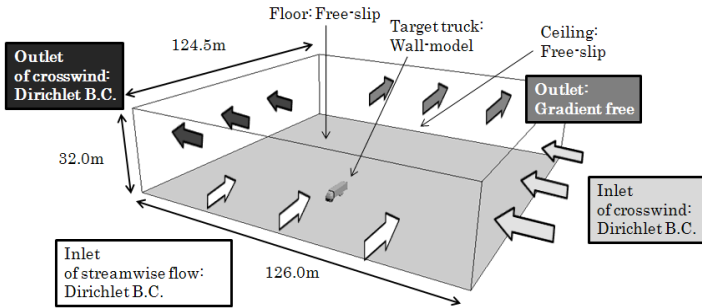


**Fig.4 Computational domain (14)**

conservation equation of momentum to avoid numerical oscillation. Additionally, the third order upwind scheme was applied only in a region upwind side of the truck, in order to avoid an overshoot of the step-like crosswind profile before it contacts with the truck. The second-order Adams–Bashforth scheme was adopted for time discretization and the time interval was set at  $5.0 \times 10^{-5}$  s. Figure 5 shows the computational grid of the present simulation. The number of vertexes is about 3.3 million and the number of elements is about 18.7 million.

Numerical simulations were conducted using the same LES code FrontFlow/red. This code was developed as part of the Frontier Simulation Software for Industrial Science (FSIS) project (15) and was optimized for HPC as part of the Revolutionary Simulation Software 21 (RSS21) project (16) supported by the Ministry of Education, Culture, Sports, Science and Technology (MEXT), Japan. Furthermore, the code was optimized for unsteady vehicle aerodynamics simulations and was extended for a coupled simulation with vehicle dynamics in a project supported by the Industrial Technology Research Grant Program in 2007 from the New Energy and Industrial Technology Development Organization of Japan (17).

The simulations were conducted on 16 nodes / 256 CPUs of a supercomputer SR11000 developed by HITACH. The coupled simulation of the fluid and vehicle dynamics for 20 seconds of physical time took about 200 hours of wall-clock time.

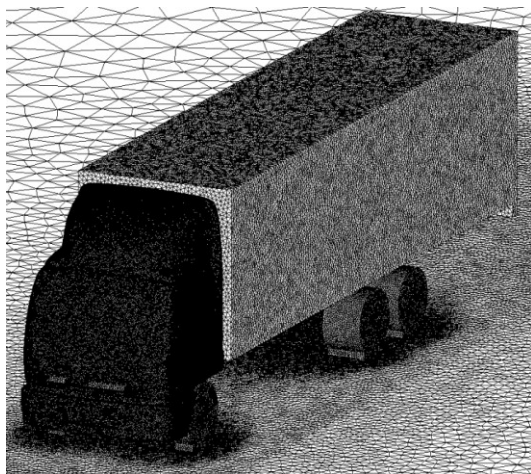


**Fig.5 Computational grids on boundary surfaces (14)**

dynamics simulation by the Arbitrary Lagrangean-Eularian (ALE) Method (9). The computational grids were deformed by assuming edges of the computational grids as spring, and the grid deformation velocity  $u_{gi}$  was considered in the fluid dynamics simulation.

### **Evaluation of Aerodynamic Forces in the Vehicle Dynamics Simulation**

In the vehicle dynamics simulation, the aerodynamic lateral force and yaw moment are given by the fluid dynamics simulation. They are simply evaluated by numerical integrations of the lateral component of a surface pressure and the yaw moment acting on the truck's body. The integrated values are substituted into  $F_w$  in equation 6 and  $M_w$  in equation 7 for the vehicle dynamics simulation at every time step.

### **ADDITIONAL SIMULATIONS FOR COMPARISONS**

#### **Vehicle Dynamics Simulation Based on a Quasi-steady Aerodynamics**

For a comparison with the coupled analysis to extract and clarify unsteady aerodynamics effects, conventional approach (7) based on a quasi-steady assumption, was also applied to evaluate the aerodynamic force and moment. The aerodynamic lateral force and yawing moment are given as

$$F_w = \frac{1}{2} C_s(\beta_w) \rho S V_R^2 \quad (11)$$

$$M_w = \frac{1}{2} C_{ym}(\beta_w) \rho S L_{wheel} V_R^2 \quad (12)$$

A crosswind velocity and aerodynamic yaw angle was observed above the center of gravity of the truck in the fluid dynamics simulation without a consideration of unsteady vehicle motion.

The coefficients of the lateral force and yawing moment in equations 11 and 12 are calculated from approximate polynomials of  $\beta_w$ , which was constructed from results of fluid dynamics simulations under several steady conditions of  $\beta_w$  from  $0^\circ$  to  $45^\circ$  in our previous study (14). In the previous simulations, the velocity imposed on the front and side boundaries were constant and the other numerical conditions, setup, and numerical code were the same as the present coupled simulation. Based on their result, the polynomial expressions became as follows:

$$C_s(\beta_w) = -4.9269 \times 10^{-9} \times \beta_w^5 + 9.3349 \times 10^{-6} \times \beta_w^3 + 1.0042 \times 10^{-1} \times \beta_w \quad (13)$$

$$C_{ym}(\beta_w) = 8.1104 \times 10^{-10} \times \beta_w^5 - 7.5480 \times 10^{-6} \times \beta_w^3 + 5.8404 \times 10^{-2} \times \beta_w \quad (14)$$

These approximate functions are drawn in Fig. 6 with plots of the results of the steady aerodynamics simulations.

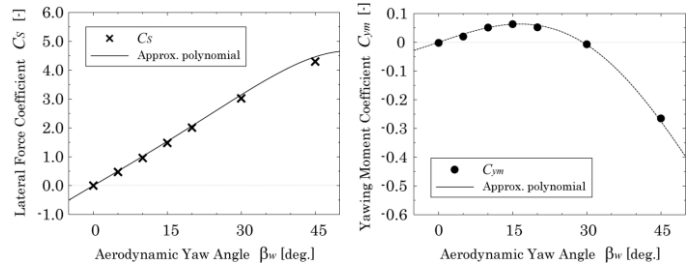


**Fig. 6 Quasi-steady aerodynamic coefficients  $C_s$  and  $C_{ym}$  and their approximate polynomials (14).**

### **One-way Coupled Simulation**

The other additional simulation was a one-way coupled simulation that considered interactions only in one-way from unsteady aerodynamics to vehicle's motion. The result can be applied to a comparison with the fully coupled analysis to extract an effect of unsteady aerodynamics caused by unsteady vehicle's motion. Therefore, vehicle's motion caused by the aerodynamics was neglected and the truck kept its constant speed and straight track in the fluid dynamics simulation, while the trajectory went off the track in the vehicle dynamics simulation. This one-way coupled simulation has been conducted and discussed in our previous study (13) and the modified simulation with higher order upwind scheme in the upstream region was newly conducted to reproduce more sharp profile in the present study.

### **RESULTS AND DISCUSSIONS**

At first, results of the fully coupled simulation of unsteady aerodynamics and vehicle dynamics of the truck subjects to sudden crosswind are mentioned and they are compared with the results of the additional simulation based on quasi-steady aerodynamics.

#### **Aerodynamics**

As a result of the fluid dynamics simulation in the fully coupled simulation, time-series of aerodynamic lateral force and yaw moment are shown in Fig.7. Results of the simulation with quasi-steady aerodynamics are also plotted in the graph.

The lateral forces  $F_w$  in Fig.7 (a) show similar profile in the two simulations, though they have a little time lag. The force monotonically increases as the truck runs into the crosswind region, and it decreases to zero as the truck goes out from the region. The time lags of the increase and the decrease between the two simulations are caused by a difference of aerodynamics evaluation. In the simulation with quasi-steady aerodynamics, the crosswind velocity and its direction are determined at the point above the gravity center of the vehicle, and the crosswind effect appears after the gravity center goes into the crosswind. While the truck is running in the crosswind, the force decreases gradually because the truck is pushed by the crosswind and the relative velocity of the crosswind is decreased by the vehicle motion.

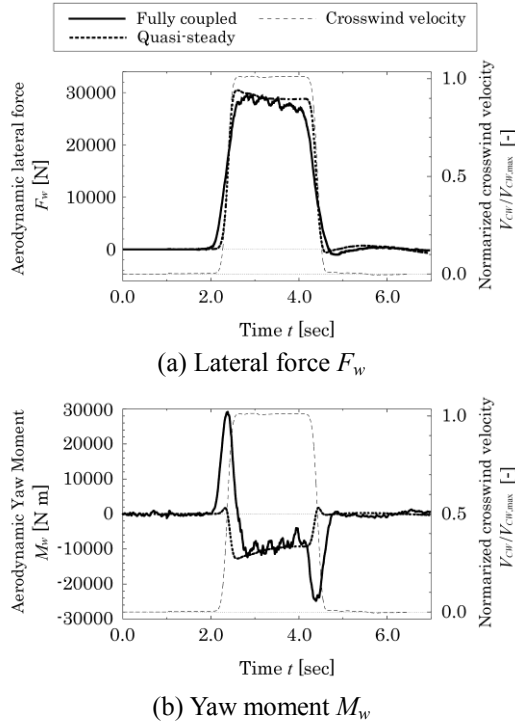
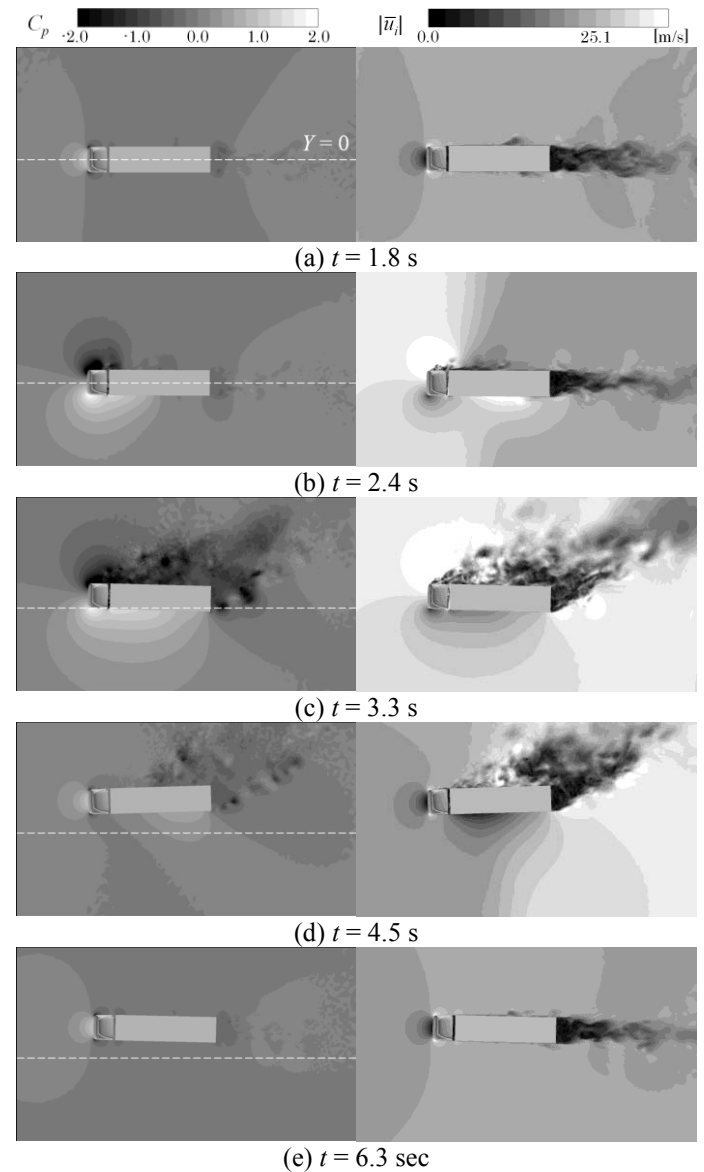


**Fig. 7 Time-series of aerodynamic force  $F_w$  and moment  $M_w$  acting on the truck**

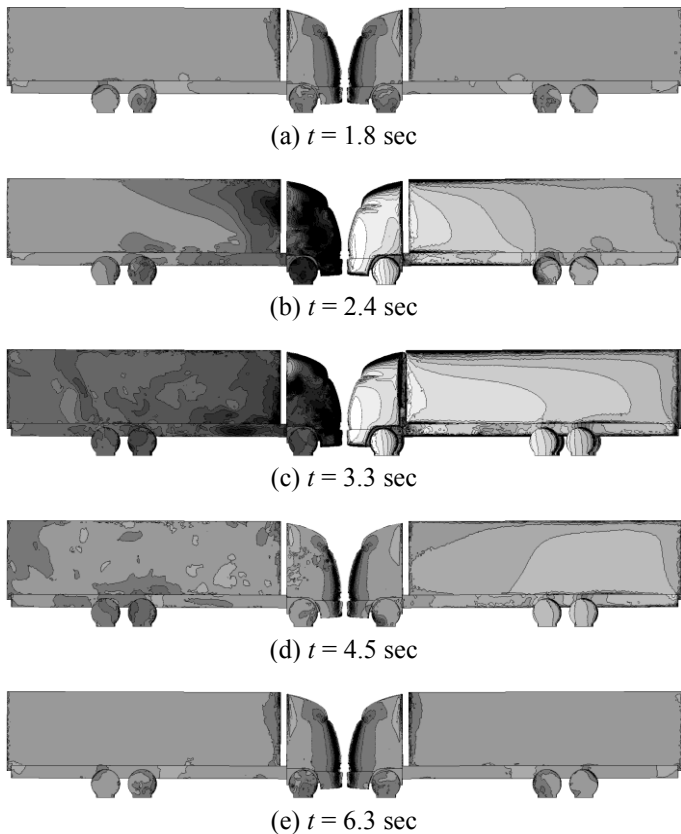
On the other hand, the yaw moments  $M_w$  in Fig.7 (b) are quite different between each simulation. In the fully coupled simulation considering the transient phenomena as the truck drives into the crosswind, the yaw moment has high positive and negative peaks as the truck drives into and out from the crosswinds, respectively. However, in the simulation with quasi-steady aerodynamics, the yawing moment shows almost monotonic increase and decrease. The peaks in the coupled simulation appear when the crosswind acts on the front half or rear half of the truck.

Figure 8 shows snapshots of the pressure and velocity fields around the truck and Fig. 9 shows the surface pressure on the lateral surface of the truck in the fully coupled simulation. Both figures give values at typical instances from 1.8 to 6.3 s. The trends of the pressure and velocity variations are qualitatively similar to those in the case of the fixed vehicle attitude, which has been simulated in the additional simulation and also in our previous study (14). The pressure distribution caused by the crosswind spreads widely on the container toward the rear. In the still air at 1.8 s, the pressure and velocity fields are almost symmetric and the truck on the track  $Y = 0$ , which is shown as white dotted lines in the figures. When the front half of the truck is subjected to the crosswind, which is shown as a high velocity magnitude, at 2.4 s, the asymmetric pressure distribution around the cabin appears although the separation on the leeward side has not been enhanced. This pressure distribution causes the high peak of aerodynamic yaw moment and it moves the track in yaw direction. The pressure also

pushes the truck in lateral direction at this moment. When the entire truck is subjected to the crosswind at 3.3 s, a large separation region appears on the leeward side and a fluctuating pressure distribution is observed on that side of the lateral surface. The high pressure region on the windward side of the truck spreads widely on the container. When the front half of the truck is exiting the crosswind at  $t = 4.5$  s, pressure on the cabin recovers its symmetric property, though the fluctuating low pressure on the leeward side caused by a remaining separation of flow. The high pressure on the windward side of the container also remains. Finally, at  $t = 6.3$  s, both pressure and velocity fields recover their symmetrical property, while the lateral displacement from the track remains yet.



**Fig. 8 Snapshots of the pressure coefficient  $C_p$  (right) and the spanwise velocity  $u_2$  (left) distributions.**



**Fig. 9 Snapshots of the pressure coefficient  $C_p$  distribution on the lateral surface of the truck. (Left: leeward side. Right: windward side.)**

### Vehicle Motion

As a result of the vehicle dynamics simulation in the fully coupled simulation, Fig.10 shows time series of the lateral course deviation  $Y$  and yaw angle  $\Psi$  of the truck. The results of the fully coupled simulation and the simulation with quasi-steady aerodynamics show qualitative difference, especially in yaw motion. The yaw motion was directly affected by the aerodynamic yawing moment, which shows particularly unsteadiness. The first responses to the crosswind had opposing directions in the yaw motion. The coupled analysis predicted positive yaw motion due to the unsteady aerodynamic yawing moment, which had a positive peak, when the vehicle is half-way into the crosswind. On the contrary, the simulation with quasi-steady aerodynamics predicted negative yaw motion due to a negative yawing moment without a high peak in the transitional situation. Regarding the lateral displacement, the first responses were also different, and the truck drifts to downstream of the crosswind more rapidly in the coupled simulation. Therefore, a trajectory of the truck in the simulation with quasi-stationary aerodynamics is smoother than the coupled simulation though the second peak of the displacement becomes larger. Quantitative difference of the maximum deviations was about 20% and the simulation with quasi-steady

aerodynamics showed greater deviation. These differences of lateral displacement and yaw motion indicate the effect of unsteady aerodynamics on vehicle motion. They are significant in the vehicle motion and the fact explains an importance to consider the unsteady aerodynamics.

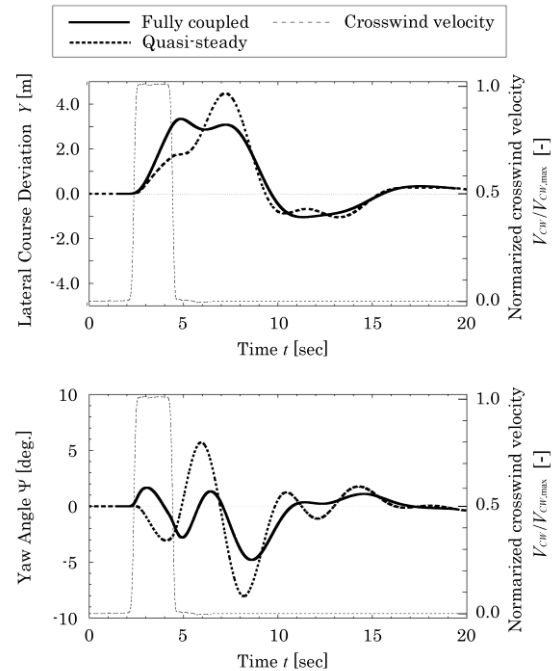


**Fig. 10 Time series of the lateral course deviations (top) and yaw angles (bottom).**

### Discussion about Unsteady Aerodynamics Effects

In the unsteady aerodynamics under crosswind condition, there are at least two kinds of phenomena related to the unsteady aerodynamics. The one is the transient aerodynamics as the truck ran into the crosswind and the other is the unsteady aerodynamics caused by unsteady vehicle's motion. In order to clarify a contribution of each phenomenon, additional simulations and comparisons were conducted.

#### Effect of Transient Aerodynamics

In order to discuss an effect of the transient aerodynamics, the one-way coupled simulation from unsteady aerodynamics to vehicle dynamics was conducted. In the one-way coupled simulation, time variation of truck's attitude was not considered in evaluations of the crosswind velocity and direction. Therefore, only the effect of transient aerodynamics as the truck drives into the crosswind can be extracted and investigated. Additionally, vehicle dynamics simulation with quasi-steady aerodynamics was also conducted under the same assumption in the crosswind velocity and direction.

The lateral displacement and yaw angles predicted in these simulations are shown in Fig.11. As same as the simulations considering the time variation of the vehicle's attitude, the displacement and yaw angle are different

qualitatively between the simulations with unsteady and quasi-steady aerodynamics. Magnitude relations of two positive peaks in the displacements are completely different in their results. Yaw angles are also different quantitatively, such as the first response to the crosswind, and the differences between the results based on the unsteady and quasi-steady aerodynamics are greater than the cases considering time variation of vehicle's attitude. This fact indicates that the transient aerodynamics as the truck drives into and out from the crosswind affects enough to the trajectory and yaw motion of the truck.

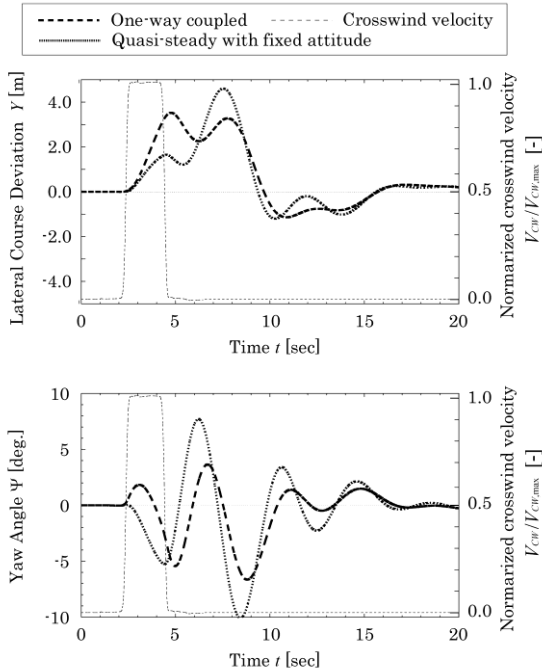


**Fig. 11 Time series of the lateral course deviations (top) and yaw angles (bottom) in one-way coupled simulation from aerodynamics to vehicle dynamics.**

**Effect of the aerodynamics induced by the vehicle's motion**

On the other hand, comparing results of the fully coupled simulation and the one-way coupled simulation, an effect of the unsteady aerodynamics induced by the unsteady vehicle motion can be discussed. Only one difference of the two simulations was consideration of the unsteady vehicle motion in the aerodynamics simulation. The comparisons of the lateral displacement and yaw angle in the two simulations are shown in Fig.12. The yaw angles show quantitative difference between the two simulations while the lateral displacements show smaller difference than the other comparisons mentioned above. Therefore, the unsteady aerodynamics induced by the unsteady vehicle motion had smaller effect on the vehicle's motion than the other unsteady aerodynamic force and moment, though it also significantly affects to the yaw motion of the truck.

In both time-series of the displacement and yaw angle, the fully coupled simulation shows smoother profiles. In that

simulation, the vehicle's attitude is changed by the aerodynamic force and moment to reduce their effect, as well as the aerodynamic damping effect. Figure 13 shows the time-series of aerodynamic moment  $M_w$  calculated in both the simulations. While the truck is running in the crosswind region, the magnitude of moment in fully coupled simulation becomes smaller than the moment in the one-way coupled simulation. This difference is caused by the lateral and yaw motions of the truck pushed by the crosswind. Since the motions decrease the relative crosswind velocity and the aerodynamic yaw angle, the aerodynamic force and moment are reduced in the fully coupled simulation.

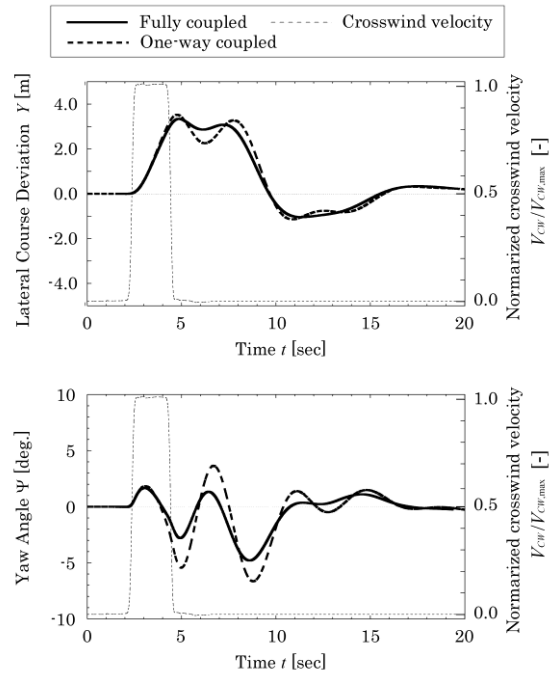


**Fig. 12 Comparisons of the lateral course deviations (top) and yaw angles (bottom) between the fully coupled and one-way coupled simulations.**

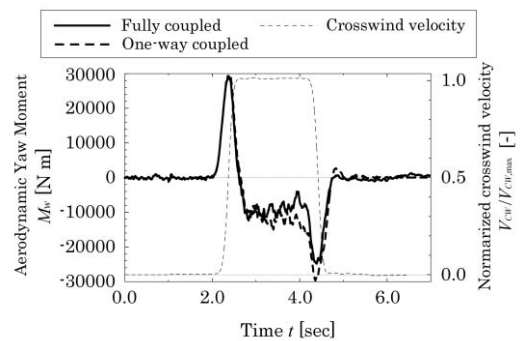


**Fig. 13 Comparisons of the aerodynamic yaw moment  $M_w$  between the fully coupled and one-way coupled simulations.**

## CONCLUSIONS

In the present study, in order to investigate how unsteady aerodynamic forces act on a vehicle subjects to a sudden crosswind, and how such transient forces affect the running or driving stability of the vehicle, the fully coupled analysis of unsteady aerodynamics and vehicle dynamics on a heavy duty truck subjected to sudden crosswinds was conducted. Large-eddy simulation with moving boundary techniques was applied to evaluate the unsteady external forces acting on the truck. The vehicle dynamics was simulated by considering horizontal motion with steering control of a driver. The results of the fully coupled simulation indicated that:

- The unsteady aerodynamics effected significantly on the motion of the truck.

The results were compared with additional simulations based on quasi-steady aerodynamics or a fixed vehicle attitude in the aerodynamics simulation. They indicated that:

- Both effects of transient aerodynamics as the truck ran into the sudden crosswind and unsteady aerodynamics induced by the unsteady vehicle's motion contributed to change the vehicle motion.
- The former effect was greater than the latter one.

As a future work for more realistic coupled simulation of the vehicle dynamics and the unsteady aerodynamics, the vehicle motion should be considered in six-degrees-of-freedom including pitch, roll, and heave motions.

## ACKNOWLEDGMENTS

This work is supported by the Industrial Technology Research Grant Program in 2007 from New Energy and Industrial Technology Development Organization (NEDO) of Japan. Part of this study was conducted using Revolutionary Simulation Software (RSS21) sponsored by the Ministry of Education, Culture, Sports, Science, and Technology, Japan.

## REFERENCES

1. Hemida, H., and Krajnović, S., 2009, "Transient Simulation of the Aerodynamic Response of a Double-Deck Bus in Gusty Winds", *J. of Fluids Eng., Trans. ASME*, vol. 131, pp. 031101-1~10
2. Aschwanden, P., Müller, J., Travaglio, G.C., Schöning, T., "The Influence of Motion Aerodynamics on the Simulation of Vehicle Dynamics," SAE Technical paper, No.2008-01-0657, 2008.
3. Okada, Y., Nouzawa, T., Nakamura, T., Okamoto, S., "Flow structures above the trunk deck of sedan-type vehicles and their influence on high-speed vehicle stability 1st report: On-road and wind-tunnel studies on unsteady flow characteristics that stabilize vehicle behavior," SAE Technical paper, No.2009-01-0007, 2009.
4. Beauvais, F.N., "Transient Nature of Wind Gust Effect on an Automobile," SAE Paper, No.670608, 1967.
5. Kobayashi, T., and Kitoh, K., 1983, "Cross-Wind Effects and the Dynamics of Light Cars", *Int. J. Veh. Des., Special Publication SP3*, pp. 142-157
6. Dominy, R. G.; Ryan, A. An Improved Wind Tunnel Configuration for the Investigation of Aerodynamic Cross Wind Gust Response. SAE paper no. 1999-01-0808, 1999.
7. Maruyama, Y. and Yamazaki, F., "Driving simulator experiment on the moving stability of an automobile under strong crosswind," *J. Wind Eng. Ind. Aerodyn.*, vol. 94, 2006, pp.191-205.
8. Tsubokura, M., Takahashi, K., Matsuuki, T., Nakashima, T., Ikenaga, T., "HPC-LES for Unsteady Aerodynamics of a Heavy Duty Truck in Wind Gust 1st report: Validation and Unsteady Flow Structures," SAE 2010 World Congress, Paper no. 2010-01-1010.
9. Smagorinsky, J., 1963, "General Circulation Experiments with the Primitive Equations, I. The Basic Experiment", *Monthly Weather Rev.*, vol.91, Num. 3, pp.99-164
10. Yoshimoto, K., "Simulation of driver-vehicle systems using a predictable model of driver's steering," *Journal of the Japan Society of Mechanical Engineering*, vol.71, no.596, 1968, pp.1181-1186 (in Japanese).
11. Hirt, C.W., Amsden, A.A., Cook, J.L., "An Arbitrary Lagrangian-Eulerian Computing Method for All Flow Speeds," *J. Comp. Phys.*, vol.14, 1974, p. 227-253.
12. Tsubokura, M., Nakashima, T., Ikenaga, T., Onishi, K., Kitoh, K., Oshima, N., and Kobayashi, T., "HPC-LES for the prediction of unsteady aerodynamic forces on a vehicle in a gusty cross-flow condition", SAE Technical paper, No. 2008-01-3001
13. Ikenaga, T., Nakashima, T., Tsubokura, M., Kitoh, K., Doi, Y., "Large-Eddy Simulation of a Vehicle Driving into Crosswind," *Review of Automotive Engineering*, vol. 31, no.1, pp.71-76.
14. Nakashima, T., Tsubokura, M., Ikenaga, T., Doi, Y., "HPC-LES for Unsteady Aerodynamics of a Heavy Duty Truck in Wind Gust - 2st report: Coupled Analysis with Vehicle Motion," SAE 2010 World Congress, Paper no. 2010-01-1021.
15. "Frontier Simulation Software for Industrial Science (FSIS)", <http://www.ciss.iis.u-tokyo.ac.jp/fsis/en/index.html>
16. "Revolutionary Simulation Software (RSS)", <http://www.ciss.iis.u-tokyo.ac.jp/rss21/en/index.html>
17. "New Energy and Industrial Technology Development Organization", <http://www.nedo.go.jp/english/index.html>